



**HAL**  
open science

## Ultra-directional source of longitudinal acoustic waves based on a two-dimensional solid/solid phononic crystal

B. Morvan, A. Tinel, Jerome O. Vasseur, R. Sainidou, P. Rembert,  
Anne-Christine Hladky, N. Swintec, P. A. Deymier

### ► To cite this version:

B. Morvan, A. Tinel, Jerome O. Vasseur, R. Sainidou, P. Rembert, et al.. Ultra-directional source of longitudinal acoustic waves based on a two-dimensional solid/solid phononic crystal. *Journal of Applied Physics*, 2014, 116 (21), pp.214901. 10.1063/1.4903076 . hal-01943205

**HAL Id: hal-01943205**

**<https://hal.science/hal-01943205>**

Submitted on 25 May 2022

**HAL** is a multi-disciplinary open access archive for the deposit and dissemination of scientific research documents, whether they are published or not. The documents may come from teaching and research institutions in France or abroad, or from public or private research centers.

L'archive ouverte pluridisciplinaire **HAL**, est destinée au dépôt et à la diffusion de documents scientifiques de niveau recherche, publiés ou non, émanant des établissements d'enseignement et de recherche français ou étrangers, des laboratoires publics ou privés.

# Ultra-directional source of longitudinal acoustic waves based on a two-dimensional solid/solid phononic crystal

Cite as: J. Appl. Phys. **116**, 214901 (2014); <https://doi.org/10.1063/1.4903076>

Submitted: 25 July 2014 • Accepted: 14 October 2014 • Published Online: 02 December 2014

B. Morvan, A. Tinel, J. O. Vasseur, et al.



View Online



Export Citation



CrossMark

## ARTICLES YOU MAY BE INTERESTED IN

[Negative refraction of acoustic waves in two-dimensional phononic crystals](#)

Applied Physics Letters **85**, 341 (2004); <https://doi.org/10.1063/1.1772854>

[Negative refraction of acoustic waves using a foam-like metallic structure](#)

Applied Physics Letters **102**, 144103 (2013); <https://doi.org/10.1063/1.4801642>

[An elastic metamaterial with simultaneously negative mass density and bulk modulus](#)

Applied Physics Letters **98**, 251907 (2011); <https://doi.org/10.1063/1.3597651>

Lock-in Amplifiers  
up to 600 MHz



Zurich  
Instruments



## Ultra-directional source of longitudinal acoustic waves based on a two-dimensional solid/solid phononic crystal

B. Morvan,<sup>1</sup> A. Tinel,<sup>1</sup> J. O. Vasseur,<sup>2</sup> R. Sainidou,<sup>1</sup> P. Rembert,<sup>1</sup> A.-C. Hladky-Hennion,<sup>2</sup> N. Swintek,<sup>3</sup> and P. A. Deymier<sup>3</sup>

<sup>1</sup>Laboratoire Ondes et Milieux Complexes, UMR CNRS 6294, Université du Havre, 75 rue Bellot, 76058 Le Havre, France

<sup>2</sup>Institut d'Electronique, de Micro-électronique et de Nanotechnologie, UMR CNRS 8520, Cité Scientifique, 59652 Villeneuve d'Ascq Cedex, France

<sup>3</sup>Department of Materials Science and Engineering, University of Arizona, Tucson, Arizona 85721, USA

(Received 25 July 2014; accepted 14 October 2014; published online 2 December 2014)

Phononic crystals (PC) can be used to control the dispersion properties of acoustic waves, which are essential to direct their propagation. We use a PC-based two-dimensional solid/solid composite to demonstrate experimentally and theoretically the spatial filtering of a monochromatic non-directional wave source and its emission in a surrounding water medium as an ultra-directional beam with narrow angular distribution. The phenomenon relies on square-shaped equifrequency contours (EFC) enabling self-collimation of acoustic waves within the phononic crystal. Additionally, the angular width of collimated beams is controlled via the EFC size-shrinking when increasing frequency. © 2014 AIP Publishing LLC. [<http://dx.doi.org/10.1063/1.4903076>]

### I. INTRODUCTION

For numerous applications of acoustic waves, it is highly desirable to produce directional sources of sound. This is particularly true in the area of underwater acoustics, where directivity of longitudinal waves is required for point-to-point communications or precise echolocation. The literature reports a variety of ways to realize directional acoustic sources.<sup>1–4</sup> In general, these sources exploit the anisotropy and/or symmetry of some heterogeneous media such as phononic crystals (PCs). These are composite structures constituted of different materials arranged in a periodic manner. For example, two dimensional PCs are typically composed of periodic arrays of cylindrical inclusions embedded in a matrix made of some other material with different elastic parameters (mass density  $\rho$  and longitudinal and transverse wave propagation velocities,  $c_l$  and  $c_t$ , respectively). The geometry and the contrast in physical and acoustical properties of the constituent materials determine the dispersive properties of PCs.<sup>5</sup> By controlling the dispersion characteristics, one can achieve peculiar properties that are not available in natural materials.<sup>6</sup> Directional acoustic sources developed so far have exploited the four-folds symmetry of square lattices of inclusions,<sup>7,8</sup> inspired by similar behavior encountered in the area of photonics (see, for instance, Ref. 9). This symmetry leads to propagation of acoustic waves constrained to specific directions. Self-collimation of acoustic beams inside the PC volume may result from the square symmetry of specific passing bands in some frequency domain.<sup>10,11</sup> In addition, the acoustic band structure of PCs can show angular band gaps that can be used as spatial filters of monochromatic sources.<sup>12,13</sup> These angular band gaps forbid the transmission of waves in some range of directions subsequently narrowing the angular distribution of acoustic beams. In this paper, we exploit both phenomena to achieve an ultra-directional sound source.

Up to date, the use of these refractive and transmission properties to produce directional acoustic sources of longitudinal waves have been demonstrated only for solid/fluid PCs.<sup>2,3,7,8,14–16</sup> These structures, constituted of solid inclusions in a fluid matrix (e.g., air or water), present several drawbacks regarding ease of handling and use in another fluid medium. Collimation in a potentially more advantageous 2D solid/solid PC has been shown but for elastic transverse waves<sup>17</sup> that cannot be supported by an external fluid medium. Here, we focus on a solid/solid PC that can be easily handled for practical applications in underwater acoustics. We demonstrate experimentally and theoretically, the possibility of constructing an efficient ultra-directional source of longitudinal waves using a PC structure made of steel rods embedded in epoxy resin matrix with a lattice constant of the order of a few mm. Some of us have previously shown<sup>19</sup> that this PC exhibits equi-frequency contours (EFCs) of quasi-square shape in some ultrasonic frequency range and consequently behaves as a self-collimator for longitudinal acoustic waves. We further analyze theoretically the related behavior and provide insights on the band structure, symmetry, and extent of EFCs, as well as the angular dependency of transmission of longitudinal waves in that PC. The EFCs show angular band gaps, which widen by increasing frequency, thus, allowing efficient angular filtering of the collimated beam. Next, underwater ultrasonic experiments are performed by introducing a primary multi-directional pinducer source at the PC center. The whole structure operates like an ultra-directional source with an emitted beam in surrounding water exhibiting a divergence of the order of just a few degrees.

The paper is organized as follows. In Sec. II, we present the fundamental, theoretically predicted, properties of the system under consideration and describe the fabricated sample and the experimental setup. Experimental results are reported and discussed in Sec. III. Excellent agreement

TABLE I. Densities and speeds of sound (longitudinal:  $c_l$  and transverse:  $c_t$ ) for the constituent materials of the PC and its surrounding medium.

Material	$\rho$ (kg/m <sup>3</sup> )	$c_l$ (m/s)	$c_t$ (m/s)
Steel	7780	5825	3227
epoxy	1180	2535	1157
water	1000	1480	...

between predictions and measurements is established and the physical mechanisms at play in the processes of collimation and spatial filtering are analyzed. Finally, conclusions are drawn in Sec. IV with some attention paid to perspectives relative to the application of this ultra-directional PC.

## II. PHONONIC CRYSTAL STRUCTURE AND EXPERIMENTAL SETUP

### A. Structure and properties

The PC consists of parallel steel cylinders of radius  $R = 1$  mm, arranged in a square lattice of lattice constant  $a = 3.23$  mm and embedded in an epoxy resin matrix. The elastic parameters for the materials considered are given in Table I. The corresponding volume filling fraction of metal rods, defined as  $\phi = \pi(R/a)^2$ , equals 0.30. The band structure of a PC assumed of infinite extent in the three dimensions is calculated using the layer-multiple-scattering technique adapted to treat 2D PC.<sup>18</sup> In the case under study, the calculation is restricted to modes, whose displacement field and wave vector lie on the  $xy$ -plane perpendicular to the inclusions (XY modes). The band structure is shown in Fig. 1(a). One observes a frequency band gap extending from 220 kHz to 390 kHz and a broad negative-slope band region ranging from 490 kHz to 650 kHz centered at the  $\Gamma$  point. The propagation modes associated with the passing band along  $\Gamma X$  direction are of longitudinal character and only longitudinal waves are—strongly—transmitted through the corresponding finite PC slab. The propagation modes associated with the passing band along  $\Gamma M$  direction are of transverse character and only in-plane transverse waves are—weakly—transmitted through the corresponding finite

PC slab. The related EFC for frequencies in a more limited interval [540, 620] kHz are shown in Fig. 1(b). The nearly square shape of the EFC and their pyramidal form with increasing frequency make this system a good candidate to achieve directionality of the propagation of elastic waves inside the PC, within that range of frequencies. Indeed all modes along the flat faces of the square EFCs possess the same group velocity, which is normal to that face. These modes carry their energy in the same direction within the same volume of the PC, which can lead to self-collimation of incident waves.<sup>10</sup> The EFCs approximate a square optimally at a frequency of 590 kHz. At that frequency, one anticipates achieving the highest degree of directionality along  $x$  and  $y$  directions perpendicular to the EFC faces.

When interested in underwater acoustic applications, one needs to consider the coupling of the PC with the surrounding medium (water), where only longitudinal waves can propagate. The size of the EFC plays, in that case, a crucial role to spatial (angular) filtering behavior of the PC immersed in water for longitudinal waves. Indeed, when passing from PC to water, the component of the wavevector parallel to the PC/water interface,  $k_{\parallel}$ , is conserved, while the total wavevector length will increase. In order to reinforce small angular aperture effect in water region, at a specific frequency and given the square EFC shape, we need to have small EFCs. This condition is fulfilled in the frequency range under study [see Fig. 1(b)]. As the EFCs shrink with increasing frequencies, angular band gaps should widen. The smaller the EFC, the narrower the range of incident angles that can be transmitted through the PC. To verify that behavior, we consider a finite PC slab of eight parallel cylinder rows, immersed in water. The slab is taken sufficiently thick to exhibit observable gap regions. In Fig. 2, we calculate<sup>18</sup> the transmittance of a longitudinal wave incident on such a slab as a function of incidence angle and for frequencies ranging from 400 kHz to 700 kHz, above the first band gap. The most important feature is the triangular shape of the angular dependency of the transmittance between 500 and 650 kHz, which demonstrates the effect of the angular band gaps. This shape is directly related to the pyramidal form of the evolution of the EFCs versus frequency [see Fig. 1(b)].

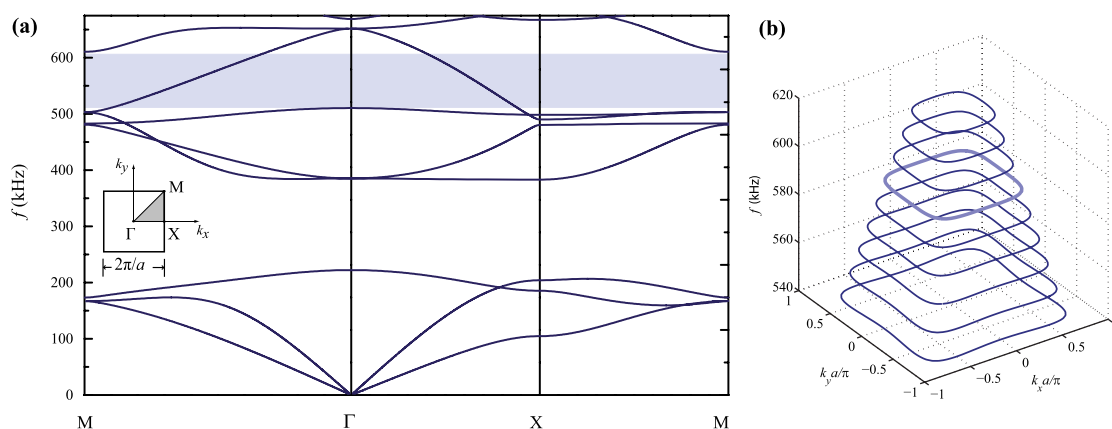


FIG. 1. (a) Calculated band structure for the steel/epoxy PC along the high symmetry directions of the first Brillouin zone (BZ). This band structure is limited to vibrational modes in the plane perpendicular to the inclusions. (b) Corresponding EFCs over the frequency range [540, 620] kHz [shaded region in (a)]; the EFC at 590 kHz is represented by a thicker line.

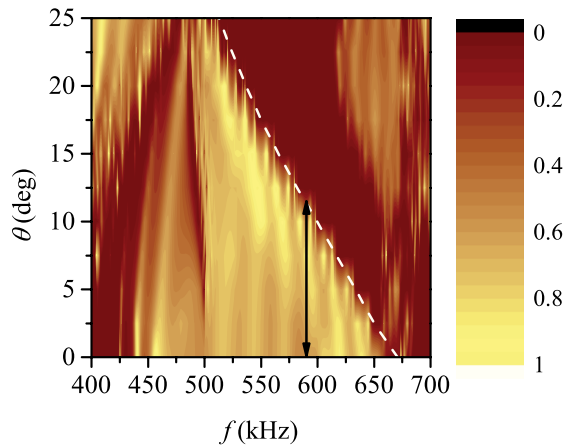


FIG. 2. Transmittance map as a function of incidence angles  $\theta$  and frequencies  $f$ , for a slab of PC consisting of eight cylinder rows, immersed in water and excited by a longitudinal incident plane wave. White dashed line denotes the upper limit of the range of permissible incident angles.

At low frequency, the edges of the EFCs are long and can therefore be coupled with longitudinal waves incident in the water region and spanning a wide range of incidence angles, leading to narrow angular band gaps. By increasing frequencies, the EFCs become smaller, restricting the range of permissible angles of incidence; the angular band gaps are now wide. The dashed white line delimits this range of permissible incident angles. For instance at the frequency of 590 kHz, where highest collimation degree is expected, transmission of an incident wave through the PC slab can only occur for angles ranging between  $0^\circ$  and approximately  $12^\circ$  (see double black arrow in Fig. 2), in accordance with the size of the square EFC. The above analysis predicts that combining collimation of waves within the PC and the small size of the EFC at a specific frequency offer the possibility of constructing an efficient ultra-directional source of longitudinal waves when a non-directional primary line-source is located at the PC center. This concept is tested experimentally below.

### B. Sample preparation

To confirm the directionality and the spatial filtering capability of the PC described previously, we have fabricated a PC sample of finite size. It consists of an array of 400 parallel cylinders of steel embedded in an epoxy resin matrix. The sample was prepared as follows. At first, a 10 cm edge cubic mold was fabricated by assembling five Plexiglas

plates. Next, 2 mm-diameter  $\times$  5 mm-deep bores, arranged in a square array, were drilled on two opposite sides of the mold to maintain the metal cylinders. Clean steel cylinders were then placed and fixed between these two plates. The liquid epoxy resin was poured in the mold and degassed during a long period of time to ensure that most of the trapped air was evacuated. After hardening, the composite material was removed from the mold and the faces of the specimen were pumiced and polished in order to obtain surfaces as smooth as possible. At the end of the sample preparation, we obtained a 80 mm-high square-base PC block ( $65.5 \text{ mm} \times 65.5 \text{ mm}$ ) containing a  $20 \times 20$  array of cylinders. To use this PC as a directional source of longitudinal acoustic waves, a 40 mm deep cylindrical hole (of diameter 2.5 mm) was drilled at the center of the sample, between four adjacent cylinders. This hole will allow, later, insertion of a non-directional ultrasonic source (see Fig. 3) used to excite the directional modes of the square EFC.

To characterize experimentally the directivity of the PC embedded source, underwater ultrasonic experiments are performed. We use as an ultrasonic source a Valpey Fisher pinducer of diameter 2.4 mm with a passband of 40 kHz centered at 590 kHz. This pinducer is introduced into the 2D PC sample via the drilled hole. The bottom of the hole is filled with an absorbing foam to avoid unwanted parasitic reflections. The detection transducer is a 1.5 in. diameter Panametrics immersion transducer with a 100% broadband centered at 500 kHz and located at 407 mm from the pinducer, i.e., a distance larger than several wavelengths to ensure the far-field assumption. The source signal is emitted with a HP 33120 A generator as a burst of 50 periods at a frequency of 590 kHz with a peak-to-peak amplitude of 150 mV with a 50 dB amplification. Using limited bursts avoids the parasitic echoes from the water tank surfaces. The transmitted signal is analyzed with a DL9140 Yokogawa oscilloscope. All temporal signals are averaged over 256 signal acquisitions. The sample and the experimental setup are shown in Fig. 3.

### III. RESULTS AND DISCUSSION

In this section, we address two aspects of the properties of the steel/epoxy PC, (1) the directionality and the spatial filtering of waves emitted by a system composed of the PC and an ultrasonic source inserted at its center, at a fixed

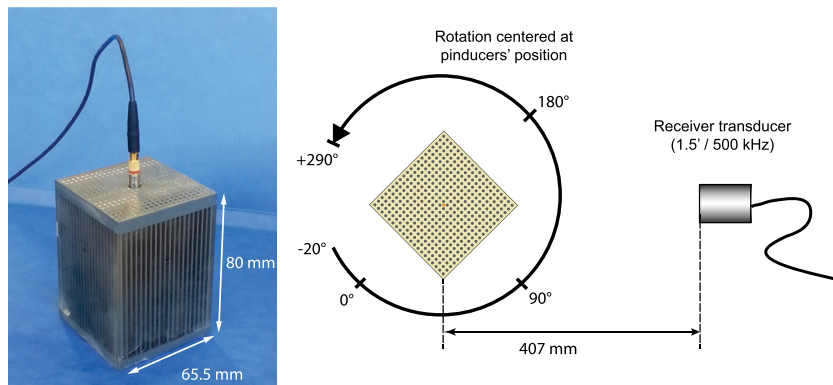


FIG. 3. The finite size PC sample with the pinducer inserted at its center (left) and the experimental setup (right). To quantify the directionality of waves emitted by the PC/Pinducer source, the receiver transducer is fixed and the PC sample is rotated by increments of  $1^\circ$  around the pinducer axis. The orientation of the pinducer remains fixed.

frequency of 590 kHz and (2) the effect of the frequency of the source on the directionality.

### A. Directionality and spatial filtering of waves

We first characterize the directionality of the pinducer ultrasonic source without the PC. The receiver transducer is fixed and the diagram of directivity is obtained by performing a rotation of the pinducer along its axis. The resulting diagram at a frequency of 590 kHz is given in Fig. 4(a). The non-circular shape of this diagram reveals that the pinducer source is not isotropic. Indeed the amplitude along the  $0^\circ$  direction is 2.5 times higher than the amplitude along the  $90^\circ$  direction. Then, the pinducer is inserted into the PC. The end of the pinducer is located at 35 mm from the top surface of the PC sample. The orientation of the pinducer is maintained at the value of  $0^\circ$  relative to the detector. The directivity properties of waves propagating through the PC and into the surrounding water are analyzed by rotating the PC with respect to its vertical axis by increments of  $1^\circ$ . The collected signals are measured at each angular position. The fact that the pinducer remains fixed allows us to overcome its anisotropy and only characterize the directionality of waves emitted through the PC. Excluding the transient part of the burst, we measure the amplitude of the transmitted signal in the steady-state regime. The resulting diagram of directivity showing the amplitude versus angular position is plotted in Fig. 4(b). We observe, as expected, the maxima of transmission in the four directions  $0^\circ$ ,  $90^\circ$ ,  $180^\circ$ , and  $270^\circ$ . This representation allows us to estimate an angular divergence of the four collimated and spatially filtered beams equal to  $\pm 4^\circ$ .

We have verified theoretically the directionality and spatial filtering ability of the finite PC immersed in water by performing finite difference time domain (FDTD) calculations.<sup>19</sup> The model system is identical to that considered experimentally. An isotropic point source is used to emit longitudinal waves at the center of the PC. This point source mimics the experimental pinducer. The calculated pressure field clearly shows self-collimation of waves inside the PC volume along the four principal directions that the group velocity can take. The experimental angular distribution of Fig. 4(b) compares well with the pressure field calculated with the FDTD method of Fig. 4(c). Both show that outside the PC, the four beams that propagate in the surrounding water exhibit a rather small spreading. The PC/pinducer system behaves as a spatial filter and can serve as a highly directional source for underwater longitudinal waves.

We note here that the transmitted signal is significantly weakened when the pinducer is inserted into the PC-block [Fig. 4(b)], compared to the corresponding radiated signal level of the pinducer immersed directly in water [Fig. 4(a)]. Of course, this level loss can be improved with an appropriate choice of the host material in order to adapt the impedance at the interface between water and host matrix (here epoxy), responsible for high level reflection when elastic waves pass across it.<sup>20</sup>

### B. Effect of frequency

In order to obtain the evolution of the directivity of wave emission versus the frequency, a fast Fourier transform is

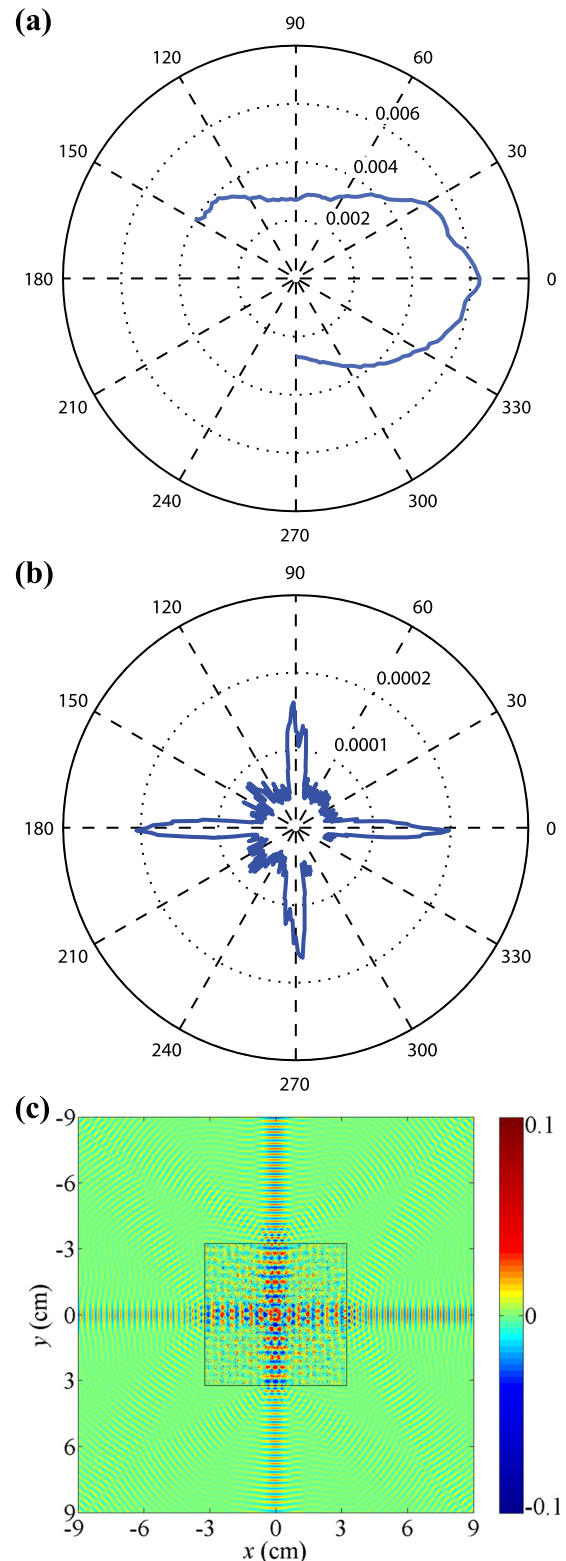


FIG. 4. Experimental maximum-amplitude (in arbitrary units) angular plot of signal received from the pinducer (a) immersed in water, (b) embedded in the PC block and immersed in water, and (c) pressure field (in arbitrary units) calculated using the FDTD method for case (b).

applied on the received signal for each angular position. Despite a single frequency burst excitation, frequency components contained in the transient part of the temporal incident signal allow us to extract information on a wide frequency band (see Fig. 5). One clearly sees the transmission-gap region

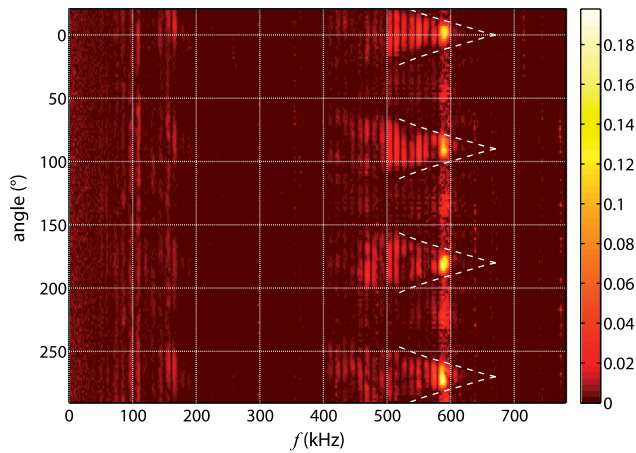


FIG. 5. Variation of experimental received pressure in the angle-frequency domain. Color scale is in arbitrary units.

extending from 200 to 400 kHz. As seen before, within the frequency region above the gap, the measured intensity of the signal is maximum at the angles  $0^\circ$ ,  $90^\circ$ ,  $180^\circ$ , and  $270^\circ$ , which corresponds to the four principal directions of transmission of the PC associated with the square symmetry of the EFCs [see Fig. 1(b)]. Maximum of transmission is obtained at a frequency of 587 kHz. Beyond this frequency, only weak non-directional transmission is observed due to the possible excitation of additional modes [see Fig. 1(a)]. The angular spread of the directed transmitted waves increases as the frequency decreases, in accordance with what we described in Subsection II A. In Fig. 5, we have drawn white lines that delimit the permissible angles that propagating waves can take (see Fig. 2). The white triangles form borders between the passing bands and the angular band gaps of the PC's

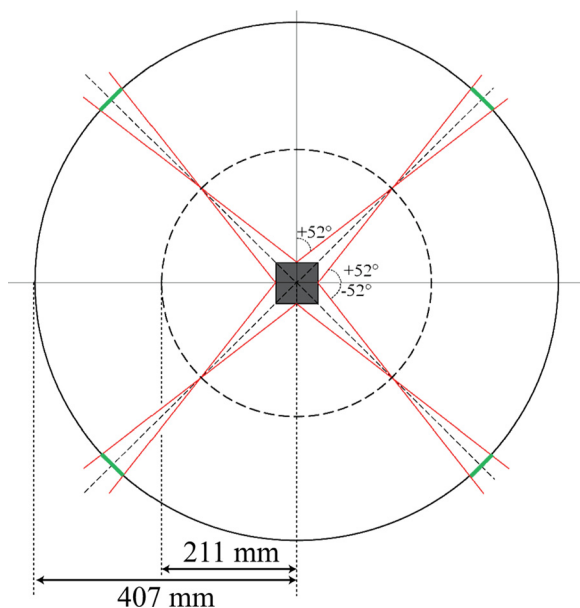


FIG. 6. Schematic of the secondary beams emerging from the PC block at angles  $\pm 52^\circ$  with respect to the normal to each face of the PC (represented as a square). The largest circle represents the position of the detector. Secondary beams from adjacent faces intersect at approximately 211 mm (dashed line circle). They form on the detection circle, extended regions with finite intensity (still lower than that of the primary directional beams) centered at the angles  $45^\circ$ ,  $135^\circ$ ,  $225^\circ$ , and  $315^\circ$ .

EFCs. As frequency increases, the angular band gaps widen narrowing the angular distribution of the beam. In addition, secondary maxima occur at angles around  $45^\circ$ ,  $135^\circ$ , and  $225^\circ$ . These maxima are particularly noticeable for frequencies near 590 kHz. They originate from the intersection of two secondary beams, each one of them emerging from adjacent faces of the PC-block at angles of  $\pm 52^\circ$  with respect to the main beam axis. The existence of these beams was reported in Ref. 19. While the primary directional beams result from the excitation of modes in the first Brillouin zone (BZ) of the PC, these secondary beams correspond to the excitation of diffracted beams of higher order, visible in Fig. 4(c). These secondary beams will intersect at a distance of  $\approx 211$  mm (almost the half of that between the center of the PC and the detector) and will form an extended region of detectable intensity at the position of the detector (see Fig. 6). The symmetry of the system leads to four of these extended detectable regions centered approximately at the angles of  $45^\circ$ ,  $135^\circ$ ,  $225^\circ$ , and  $315^\circ$ . Only three of these extended regions are observable in Fig. 5 due to geometrical constraints imposed by our experimental setup.

#### IV. CONCLUSIONS

We have studied theoretically and experimentally the directivity properties of acoustic waves for a 2D PC made of a square array of steel cylinders embedded in epoxy matrix in which we inserted a non-directional ultrasonic pinducer source. The whole PC/pinducer structure is immersed in water. In particular, we demonstrated that this system serves as an ultra-directional source of longitudinal waves in the surrounding medium, near the frequency of 590 kHz. The phenomenon relies on square-shaped EFCs of the corresponding PC in the frequency range [500, 600] kHz, which shrink by increasing frequency. Consequently, collimation of acoustic waves takes place together with angular filtering of the acoustic beam in the water region. By symmetry, four such narrow beams are emitted by the system. These intense primary beams are accompanied by significantly weaker secondary ones (resulting from higher order diffraction) that affect only marginally the performance of the PC/pinducer system as ultra-directional source of acoustic waves. This study opens interesting perspectives in the design of source of acoustic waves for underwater applications by taking advantage of the unique characteristics of PCs. In particular, the ability to engineer the band structures of PCs gives a tremendous advantage in the design of spatial filters and directional sources of acoustics waves.

<sup>1</sup>Liang-Shan Chen, Chao-Hsien Kuo, and Z. Ye, "Acoustic imaging and collimating by slabs of sonic crystals made from arrays of rigid cylinders in air," *Appl. Phys. Lett.* **85**, 1072 (2004).

<sup>2</sup>C. Qiu and Z. Liu, "Acoustic directional radiation and enhancement caused by band-edge states of two-dimensional phononic crystals," *Appl. Phys. Lett.* **89**, 063106 (2006).

<sup>3</sup>C. Qiu, Z. Liu, J. Shi, and C. T. Chan, "Directional acoustic source based on the resonant cavity of two-dimensional phononic crystals," *Appl. Phys. Lett.* **86**, 224105 (2005).

<sup>4</sup>A. Håkansson, D. Torrent, F. Cervera, and J. Sánchez-Dehesa, "Directional acoustic source by scattering acoustical elements," *Appl. Phys. Lett.* **90**, 224107 (2007).

<sup>5</sup>Y. Pennec, J. O. Vasseur, B. Djafari-Rouhani, L. Dobrzynski, and P. A. Deymier, "Two-dimensional phononic crystals: Examples and applications," *Surf. Sci. Rep.* **65**, 229 (2010).

- <sup>6</sup>In *Acoustic Metamaterials and Phononic Crystals*, Springer Series in Solid-State Sciences Vol. 173, edited by P. A. Deymier (Springer, Berlin, 2013).
- <sup>7</sup>J. Mei, C. Qiu, J. Shi, and Z. Liu, "Enhanced and directional water wave emission by embedded sources," *Wave Motion* **47**, 131 (2010).
- <sup>8</sup>Tsung-Tsong Wu, Chung-Hao Hsu, and Jia-Hong Sun, "Design of a highly magnified directional acoustic source based on the resonant cavity of two-dimensional phononic crystals," *Appl. Phys. Lett.* **89**, 171912 (2006).
- <sup>9</sup>S. Enoch, B. Gralak, and G. Tayeb, "Enhanced emission with angular confinement from photonic crystals," *Appl. Phys. Lett.* **81**, 1588 (2002).
- <sup>10</sup>J. Bucay, E. Roussel, J. O. Vasseur, P. A. Deymier, A.-C. Hladky-Hennion, Y. Pennec, K. Muralidharan, B. Djafari-Rouhani, and B. Dubus, "Positive, negative, zero refraction, and beam splitting in a solid/air phononic crystal: Theoretical and experimental study," *Phys. Rev. B* **79**, 214305 (2009).
- <sup>11</sup>V. Espinosa, V. J. Sánchez-Morcillo, K. Staliunas, I. Pérez-Arjona, and J. Redondo, "Subdiffractive propagation of ultrasound in sonic crystals," *Phys. Rev. B* **76**, 140302(R) (2007).
- <sup>12</sup>R. Picó, I. Pérez-Arjona, V. J. Sánchez-Morcillo, and K. Staliunas, "Evidences of spatial (angular) filtering of sound beams by sonic crystals," *Appl. Acoust.* **74**, 945 (2013).
- <sup>13</sup>V. Romero-García, R. Picó, A. Cebrecos, K. Staliunas, and V. J. Sanchez-Morcillo, "Angular band gaps in sonic crystals: Evanescent waves and spatial complex dispersion relation," *J. Vib. Acoust.* **135**, 041012 (2013).
- <sup>14</sup>Z. Wang, P. Zhang, Y. Zhang, and X. Nie, "Experimental verification of directional liquid surface wave emission at band edge frequencies," *Physica B* **431**, 75 (2013).
- <sup>15</sup>Feng-Chia Hsu, Tsung-Tsong Wu, Jin-Chen Hsu, and Jia-Hong Sun, "Directional enhanced acoustic radiation caused by a point cavity in a finite size two-dimensional phononic crystal," *Appl. Phys. Lett.* **93**, 201904 (2008).
- <sup>16</sup>J. Mei, C. Qiu, J. Shi, and Z. Liu, "Highly directional liquid surface wave source based on resonant cavity," *Phys. Lett. A* **373**, 2948 (2009).
- <sup>17</sup>W. Liu and X. Su, "Collimation and enhancement of elastic transverse waves in two-dimensional solid phononic crystals," *Phys. Lett. A* **374**, 2968 (2010).
- <sup>18</sup>R. Sainidou, P. Rembert, J. O. Vasseur, and A.-C. Hladky-Hennion, "The layer-multiple-scattering method as applied to two-dimensional phononic crystals," in *Proceedings of Phononics 2013: 2nd International Conference on Phononic Crystals/Metamaterials, Phonon Transport and Optomechanics, Sharm El-Sheikh, Egypt, 2-7 June 2013*.
- <sup>19</sup>N. Swintec, J. O. Vasseur, A. C. Hladky-Hennion, C. Croëne, S. Bringuier, and P. A. Deymier, "Multifunctional solid/solid phononic crystal," *J. Appl. Phys.* **112**, 024514 (2012).
- <sup>20</sup>The elastic parameters mismatch between water and epoxy is due to the difference in the longitudinal velocity (the mass densities are close to each other). One should use a polymer matrix, whose longitudinal velocity approaches that of water (of the order of 1500 m/s) and with the same Poisson ratio as that of the epoxy ( $\nu = 0.36$ ). Such a material still ensures a band structure of the same form as the one shown in Fig. 1, although shifted at lower frequencies (the frequency axis of the dispersion plot is multiplied by a factor  $1500/2535 \approx 0.6$ ; the operating frequency 590 kHz is now shifted to 350 kHz). As an example, one can consider Nyrim<sup>®</sup> 1525 (see <http://www.matweb.com>).